



# Secondary Data Analytics of Aquaporin Expression Levels in Glioblastoma Stem-Like Cells

## Citation

Isokpehi, Raphael D, Katharina C Wollenberg Valero, Barbara E Graham, Maricica Pacurari, Jennifer N Sims, Udensi K Udensi, and Kenneth Ndebele. 2015. "Secondary Data Analytics of Aquaporin Expression Levels in Glioblastoma Stem-Like Cells." *Cancer Informatics* 14 (1): 95-103. doi:10.4137/CIN.S22058. <http://dx.doi.org/10.4137/CIN.S22058>.

## Published Version

doi:10.4137/CIN.S22058

## Permanent link

<http://nrs.harvard.edu/urn-3:HUL.InstRepos:21462356>

## Terms of Use

This article was downloaded from Harvard University's DASH repository, and is made available under the terms and conditions applicable to Other Posted Material, as set forth at <http://nrs.harvard.edu/urn-3:HUL.InstRepos:dash.current.terms-of-use#LAA>

## Share Your Story

The Harvard community has made this article openly available.  
Please share how this access benefits you. [Submit a story](#).

[Accessibility](#)

# Secondary Data Analytics of Aquaporin Expression Levels in Glioblastoma Stem-Like Cells



Raphael D. Isokpehi<sup>1</sup>, Katharina C. Wollenberg Valero<sup>1</sup>, Barbara E. Graham<sup>2,3</sup>, Maricica Pacurari<sup>4</sup>, Jennifer N. Sims<sup>2</sup>, Udensi K. Udensi<sup>3</sup> and Kenneth Ndebele<sup>2,3,5</sup>

<sup>1</sup>College of Science, Engineering, and Mathematics, Bethune-Cookman University, Daytona Beach, FL, USA. <sup>2</sup>Laboratory of Cancer Immunology, Target Identification and Validation, Department of Biology, Jackson State University, MS, USA. <sup>3</sup>NIH RCMI-Center for Environmental Health, College of Science, Engineering, and Technology, Jackson State University, Jackson, MS, USA. <sup>4</sup>Department of Biology, Jackson State University, MS, USA. <sup>5</sup>Department of Pathology, Harvard Medical School, Beth Israel Deaconess Medical Center, Boston, MA, USA.

**ABSTRACT:** Glioblastoma is the most common brain tumor in adults in which recurrence has been attributed to the presence of cancer stem cells in a hypoxic microenvironment. On the basis of tumor formation *in vivo* and growth type *in vitro*, two published microarray gene expression profiling studies grouped nine glioblastoma stem-like (GS) cell lines into one of two groups: full (GSf) or restricted (GSr) stem-like phenotypes. Aquaporin-1 (AQP1) and aquaporin-4 (AQP4) are water transport proteins that are highly expressed in primary glial-derived tumors. However, the expression levels of AQP1 and AQP4 have not been previously described in a panel of 92 glioma samples. Therefore, we designed secondary data analytics methods to determine the expression levels of AQP1 and AQP4 in GS cell lines and glioblastoma neurospheres. Our investigation also included a total of 2,566 expression levels from 28 Affymetrix microarray probe sets encoding 13 human aquaporins (AQP0–AQP12); CXCR4 (the receptor for stromal cell derived factor-1 [SDF-1], a potential glioma stem cell therapeutic target); and PROM1 (gene encoding CD133, the widely used glioma stem cell marker). Interactive visual representation designs for integrating phenotypic features and expression levels revealed that inverse expression levels of AQP1 and AQP4 correlate with distinct phenotypes in a set of cell lines grouped into full and restricted stem-like phenotypes. Discriminant function analysis further revealed that AQP1 and AQP4 expression are better predictors for tumor formation and growth types in glioblastoma stem-like cells than are CXCR4 and PROM1. Future investigations are needed to characterize the molecular mechanisms for inverse expression levels of AQP1 and AQP4 in the glioblastoma stem-like neurospheres.

**KEYWORDS:** aquaporins, aquaporin-1, aquaporin-4, brain, cancer, gliomas, glioblastoma, hypoxia, neurospheres, visual analytics

**CITATION:** Isokpehi et al. Secondary Data Analytics of Aquaporin Expression Levels in Glioblastoma Stem-Like Cells. *Cancer Informatics* 2015;14:95–103 doi: 10.4137/CIN.S22058.

**RECEIVED:** November 20, 2014. **RESUBMITTED:** June 01, 2015. **ACCEPTED FOR PUBLICATION:** June 04, 2015.

**ACADEMIC EDITOR:** J.T. Efrid, Editor in Chief

**TYPE:** Original Research

**FUNDING:** This work was funded by the Office of the Provost, Bethune-Cookman University; the National Institutes of Health (NIH/NIMHD G12MD007581, NIH/NIMHD 1P20MD006899, NIH/NIGMS 5T32GM095335); and the National Science Foundation (NSF-HRD-1435186). The authors confirm that the funder had no influence over the study design, content of the article, or selection of this journal.

**COMPETING INTERESTS:** Authors disclose no potential conflicts of interest.

**CORRESPONDENCE:** isokpehir@cookman.edu

**COPYRIGHT:** © the authors, publisher and licensee Libertas Academica Limited. This is an open-access article distributed under the terms of the Creative Commons CC-BY-NC 3.0 License.

Paper subject to independent expert blind peer review by minimum of two reviewers. All editorial decisions made by independent academic editor. Upon submission manuscript was subject to anti-plagiarism scanning. Prior to publication all authors have given signed confirmation of agreement to article publication and compliance with all applicable ethical and legal requirements, including the accuracy of author and contributor information, disclosure of competing interests and funding sources, compliance with ethical requirements relating to human and animal study participants, and compliance with any copyright requirements of third parties. This journal is a member of the Committee on Publication Ethics (COPE).

Published by Libertas Academica. Learn more about this journal.

## Introduction

Water transport channel proteins, referred to as aquaporins, primarily facilitate the transport of water across biological membranes in various cell types and organisms.<sup>1–5</sup> We have previously compared the tissue expression of aquaporins of mammals (human, mouse, and rat) and chicken using data from expressed sequence tags (ESTs).<sup>4</sup> Here we report a computational evaluation of the expression levels of human aquaporins (AQP0–AQP12) in 92 glioma samples consisting of human glioblastoma stem-like (GS) cell lines, conventional glioma cell lines, and primary tumors.<sup>6,7</sup> Based on tumor formation *in vivo* and growth type *in vitro*, two microarray gene expression profiling studies grouped nine GS cell lines into one of two groups: full (GSf) or restricted (GSr) stem-like phenotypes.<sup>6,7</sup> Aquaporin-1 (AQP1) and aquaporin-4 (AQP4) are highly expressed in primary tumors. However, the expression levels of AQP1 and AQP4 were not described in the two publications that analyzed expression levels of genes in a panel

of 92 glioma samples. Therefore, we designed secondary data analytics methods to determine the expression levels of AQP1 and AQP4 in GS cell lines and glioblastoma neurospheres.

The motivation for the investigation is the emerging knowledge on the role of cancer stem cells in glioblastoma.<sup>7–10</sup> Glioblastoma is the most common brain tumor in adults<sup>11</sup> described as highly invasive; heterogeneous phenotypes; high rate of recurrence after treatment; poor prognosis; and a median survival time of approximately 15 months.<sup>12–14</sup> The recurrence has been attributed to the presence of cancer stem cells.<sup>15</sup> We are particularly interested in the expression of aquaporins in neurospheres (glioblastoma clonogenic cells), which are induced by hypoxia and represent the most malignant zones of glioblastomas.<sup>9</sup>

We have integrated methods of data transformation, visual representation of data, and statistical analyses to compare the expression levels of aquaporins in a panel of 92 glioma cells. A key finding was a pattern of inverse expression levels of



AQP1 and AQP4 probe sets in the datasets from GS cell lines and neurospheres. Interactive visual representation designs for integrating phenotypic features and expression levels revealed that inverse expression levels of AQP1 and AQP4 correlated with distinct phenotypes in a set of cell lines grouped into full and restricted stem-like phenotypes. Our analysis also included expression levels of CXCR4 (the receptor for stromal cell derived factor-1 [SDF-1], a potential glioma stem cell therapeutic target), and PROM1 (prominin-1 gene encoding CD133, the widely used glioma stem cell marker). In the dataset analyzed, discriminant function analysis revealed that AQP1 and AQP4 expression levels are better predictors for tumor formation and growth types in GS cells than are CXCR4 and PROM1. The methods developed included visual representations of statements on the expression levels and phenotypic characteristics of glioblastoma in two articles.<sup>6,7</sup> This form of secondary data analysis of statements in publications on glioblastoma could uncover scientific discoveries of therapeutic significance and thus be relevant beyond the scope of this article. Future investigations are needed to characterize the molecular mechanisms for inverse expression levels of AQP1 and AQP4 in the glioblastoma stem-like neurospheres.

## Materials and Methods

**Overview.** We have analyzed gene expression for human aquaporins (AQP0–AQP12), CXCR4, and PROM1. In the data analytics procedure, gene expression and phenotypic data were collected from online repositories and transformed for visual analytics (interactive visual representations) and statistical analysis (multivariate analysis, for example discriminant function analysis [DFA]). Selected statements in publication describing the glioblastoma samples were evaluated in the visual representations. Prognostic ratios describing observations are then proposed.

**Gene expression data.** Gene expression data on glioma cancer cell samples were obtained from the BIOGPS dataset 1692 (<http://biogps.org/dataset/1692/>).<sup>16</sup> The microarray platform was Affymetrix Human Genome U133 Plus 2.0 Array. The BIOGPS provides a gene-centric view across all the 92 samples in the Gene Expression Omnibus (GEO) Series (GSE23806) consisting of human Glioblastoma Stem-like (GS) cell lines, conventional glioma cell lines, and primary tumors.<sup>6,7</sup> This view does not provide a visual representation of the expression of gene sets: for example, all human aquaporin gene family. Such a comprehensive view of the expression data would be useful for developing new hypotheses on the expression and localization of human aquaporins in glioma cancers. The Log<sub>2</sub> GeneChip Robust Multiarray Averaging (gcRMA) processed signals (expression data) for Affymetrix probe set(s) mapped to the each aquaporin gene were downloaded from BIOGPS for visual analytics.

**Data preparation and design of visual representations.** The availability of a wealth of data from biological research on glioblastoma, including expression of genes and localization of proteins as well as heterogeneity of glioblastoma types,

presents opportunities for secondary data analytics using visual analytics tools. Visual analytics, the science of analytical reasoning via visual interactive interfaces, can be used to build knowledge from data, make sense of the data, and make decisions from data for future research.<sup>17–19</sup> In this study, we used visual analytics to focus the analysis of the datasets.

Gene expression values for the 13 human aquaporins (AQP0–AQP12), CXCR4, and PROM1 in glioma cancer cell samples (GSM198765–GSM198781 and GSM587155–GSM587229) were used to construct visual representations of data on expression levels. The expression-level data (Log<sub>2</sub> gcRMA processed signal data) for each aquaporin consist of columns of 92 tissue samples (GSM series) and the probe set(s). The dataset for each aquaporin was transformed into three columns (Tissue, Probeset [abbreviation for probe set], and Value) using the Tableau Reshape Tool (Tableau Software) in Microsoft Excel (Microsoft Corporation). The corresponding AQP symbol was then included in the final dataset, which consisted of four columns, namely, AQP, Tissue, Probeset, and Value. The number of rows in a dataset is equal to the number of probe sets multiplied by 92. Therefore a gene with two probe sets will have 184 rows of data following the headers.

All 15 data files were uploaded in an additive manner in Tableau Desktop Professional (Tableau Software) and then used to construct a dataset used for visual analytics. A second dataset consisted of 1) the metadata on the 92 tissue samples that included the title of the sample and cell type,<sup>16</sup> and 2) the metadata on the tumor formation *in vivo* and growth type *in vitro* of the GS cells.<sup>7</sup> The annotation of the cell lines included age, sex, location of tumor, the recurrence of the tumor, and results of p53 assays and TP53 mutations. The tumor formation types were no tumor, diffuse and solid tumors, while the growth types were adherent, semi-adherent, and spheres.

A visual representation design was developed to display the expression values of the genes in columns and the corresponding glioma samples (GSM198765–GSM198781 and GSM587155–GSM587229) in rows. An interactive box plot representation was also developed to compare the expression levels of the 15 genes. The visual representations were further grouped based on the unsupervised hierarchical cluster analysis (described by Schulte et al.<sup>6</sup>) into primary tumors, GSf, GSr, conventional cell lines, and monolayer cultures. A heat map representation was developed to compare the GSf and GSr samples. The GS cells GS-3 and GS-7 lineage were selected for analytics since the publication describing CXCR4 as a therapeutic target used clonal sublines from GS-3 and GS-7 to test for phenotypic stability of clones to parental lines.<sup>6</sup> GS-3 had the full stem-like phenotype (GSf), while GS-7 had the restricted stem-like phenotype (GSr). Since neurospheres (glioblastoma clonogenic cells) are induced by hypoxia and represent the most malignant zones of glioblastomas,<sup>9</sup> we compared the expression levels of AQP1, AQP4, CXCR4, and PROM1 in neurosphere samples. Statements in



the article by Schulte and colleagues<sup>6</sup> on phenotypes and gene expression profiles of glioblastoma samples were evaluated in the visual representations reported here.

**Statistical analysis of gene expression data.** The dataset for statistical analysis consisted of 1) the glioma cell identifier (starting with GSM), 2) title of glioma cell, tumor formation, and 3) gene expression values for AQP0–AQP12, CXCR4, and PROM1. To test for differences of AQP expression between different categories of *in vitro* growth type and tumor formation *in vivo*, a multifactorial Kruskal–Wallis ANOVA was performed in STATISTICA (StatSoft) over all cell lines. Test-wide Bonferroni correction was applied to account for multiple variable comparisons. Categories for growth type were conventional cell line expression, primary tumor expression, adherent cell culture expression, semi-adherent cell culture expression, and spherical cell culture expression. Categories for *in vivo* tumor formation were diffuse, solid, and no tumor. Additionally, primary tumor was a separate category to account for the obviously different expression patterns between primary tumor and subsequent cell lines. Expression patterns per test were furthermore loosely grouped into HIGH, medium (MED), and LOW expression according to the group expression mean. An additional Kruskal–Wallis ANOVA was performed between AQP1 and AQP4 levels averaged per cell line, and the averaged expression levels of two additional tumor markers CXCR4 and PROM1 (results not shown), and these markers were assigned to LOW, medium (MED), and HIGH expression patterns. Discriminant Function Analysis was then performed over all four markers to test whether *in vivo* tumor formation and *in vitro* growth type could be predicted by the expression of all four markers.

## Results

**Inverse expression levels of AQP1 and AQP4 in glioblastoma stem-like cells.** A new dataset on the expression levels of probe sets of the aquaporin genes CXCR4 and PROM1 (CD133) was constructed from raw data downloaded for each gene in the BIOGPS dataset 1692 (<http://biogps.org/dataset/1692/>). The constructed dataset, available as a tab in the supplementary spreadsheet file, consisted of a total of 2,566 expression values for 28 Affymetrix probe sets encoding 13 human aquaporins (AQP0–AQP12), CXCR4, and PROM1. In Figure 1, a visual representation is shown of the expression values of all the probe sets in glioblastoma stem-like cells (GS-1 to GS-12) grouped by phenotype (full or restricted). A box plot was constructed from the expression levels of the 15 genes in the GS-3 and GS-7 lineages (Fig. 2). The highest levels of expression were found in the probe sets of AQP1, AQP4, and CXCR4. The plot was annotated for potentially interesting expression levels that were outliers or at the extreme levels of the box. Inverse expression levels of AQP1 and AQP4 were observed between the full (GS-3) and restricted (GS-7) GS cells.

We found agreement between the statements in the publication on the phenotypic stability of two lineages of glioma stem-like cells (GS-3 and GS-7) and our visual representation. Thus in Figure 3, the visual representation (heat map) shows the expression levels for AQP1, AQP4, CXCR4, and PROM1 in two clonal sublines (GS-3 and GS-7) and their associated passaged parental lines and neurospheres.

The following statements were evaluated in the visual representation: “All GS-3 sublines grew spherically, expressed CD133 and formed invasive tumors in nude mice, phenocopying the parental line. GS-7 subclones behaved more variably: Clone 3 grew semiadherent like the parental line, whereas Clones 1 and 2 grew spherically, a distinction reflected also in the more closely related expression profiles of Clones 1 and 2 versus Clone 3 and parental GS-7 cells.”<sup>6</sup>

The heat map visual representation (Fig. 3) revealed an inverse relationship of AQP1 and AQP4 expression levels in the full (GSf, GS-3) and restricted (GSr, GS-7) GS cells. The ranges of expression levels for AQP1 were 1.46–3.44 for GS-3 cells and 1.64–7.75 for GS-7 cells. The average of the expression levels across the 92 glioma samples for the two AQP1 probe sets was 4.55. In the case of AQP4, the ranges were 3.5–11.06 for GS-3 cells and 1.72–3.56 for GS-7 cells. The average expression level for the five AQP4 probe sets across the 92 glioma samples was 4.28. In the GS-7 cells, the expression level of CXCR4 was distinct for clones 1 and 2 compared to clone 3 (Fig. 3).

Another set of statements evaluated using visual representations (Fig. 4) was: “In conclusion, the group of GSf cell lines emerges as a more representative model for human glioblastomas than other GS lines or conventional glioma cell lines, mirroring original tumor gene expression signatures most closely and maintaining highly invasive growth *in vivo* as well as stem cell characteristics *in vitro*.”<sup>6</sup>

In Figure 4, the expression levels of AQP1, AQP4, CXCR4, and PROM1 probe sets for 17 neurospheres samples (8 GSf and 9 GSr) are compared using a heat map that includes the expression values. The probe set selected for each gene was that with the highest total expression level compared to other probe sets. Therefore, probe sets 209047\_at (AQP1), 226228\_at (AQP4), 217028\_at (CXCR4), and PROM1 (204304\_s\_at) were selected for comparison (Fig. 4). We used the unpaired two-tailed *t*-test to determine the statistical significance of the difference between the means of the ratios of AQP1/AQP4 for GSf and GSr neurosphere samples. The two-tailed *P*-value equaled 0.0008; therefore the difference between the ratios of GSf and GSr was considered highly significant. The heat map visual representation revealed groups of neurospheres by color coding of the probe set expression values. The GSf neurospheres grouped into four groups based on similarity of heat map color coding: Group A (GS-9-2, GS-3-2, and GS-3); Group B (GS-9); Group C (GS-8-2, GS-5-2, GS-5); and Group D (GS-8). Group D neurosphere (GS-8) did not follow the inverse gene expression levels of low AQP1 ( $\leq 6.0$ ) and high AQP4 ( $> 6.0$ ) (Fig. 4).

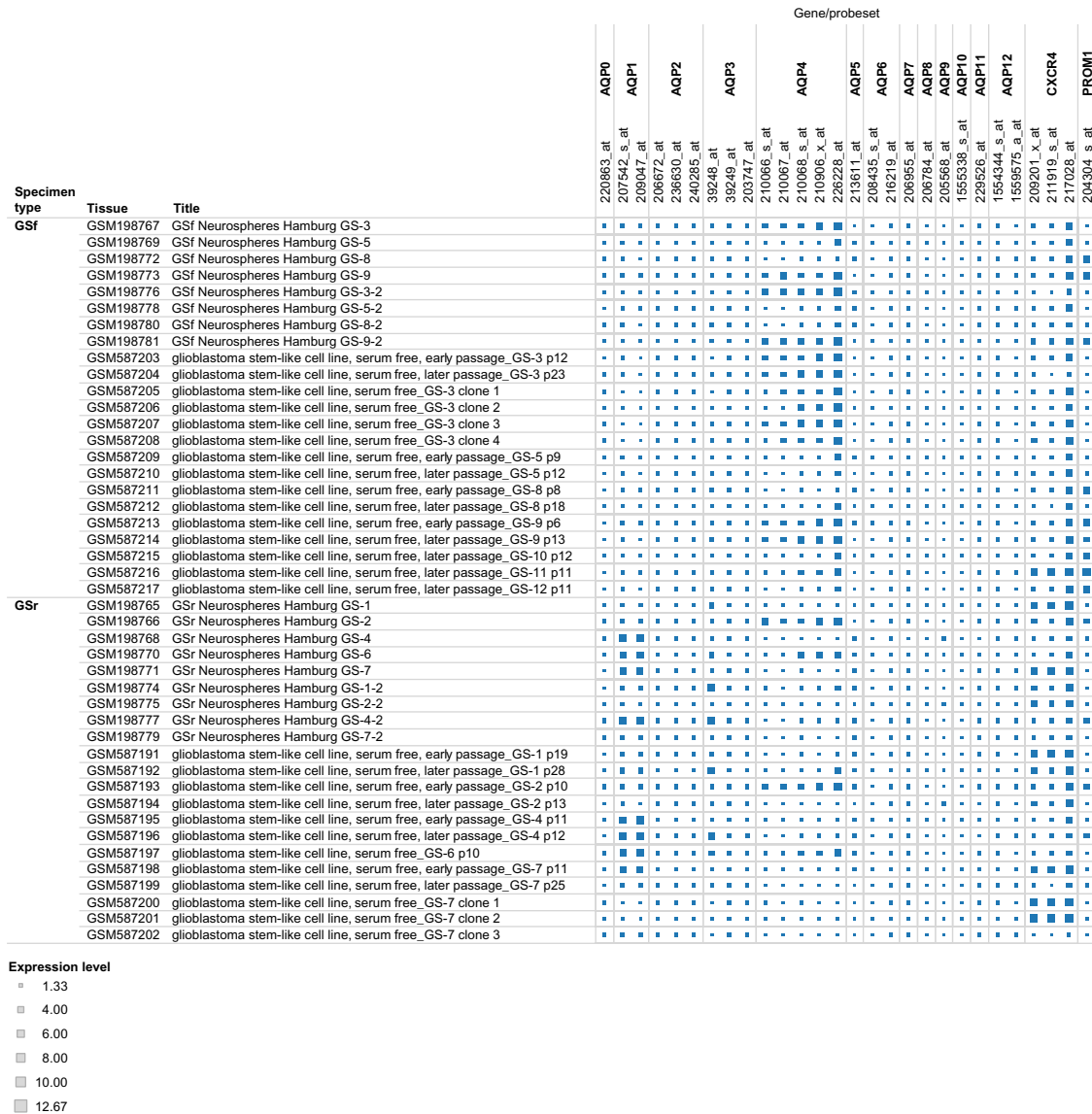


**Figure 1.** Expression levels of all the probe sets in glioblastoma stem-like cells (GS1–GS-12) grouped by phenotype (full or restricted). Interactive version of figure is available at [https://public.tableausoftware.com/views/glioma\\_aqp/figure1](https://public.tableausoftware.com/views/glioma_aqp/figure1).

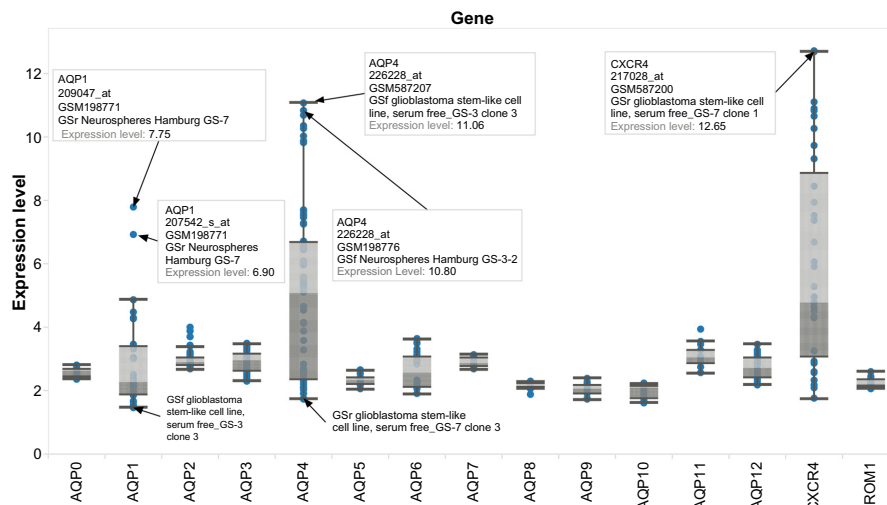


**Figure 2.** Box plot of expression levels for AQP1, AQP4, CXCR4, and PROM1 in two glioblastoma stem-like clonal sublines (GS-3 and GS-7) and their associated passaged parental lines and neurospheres. Interactive version of figure is available at [https://public.tableausoftware.com/views/glioma\\_aqp/figure2](https://public.tableausoftware.com/views/glioma_aqp/figure2).

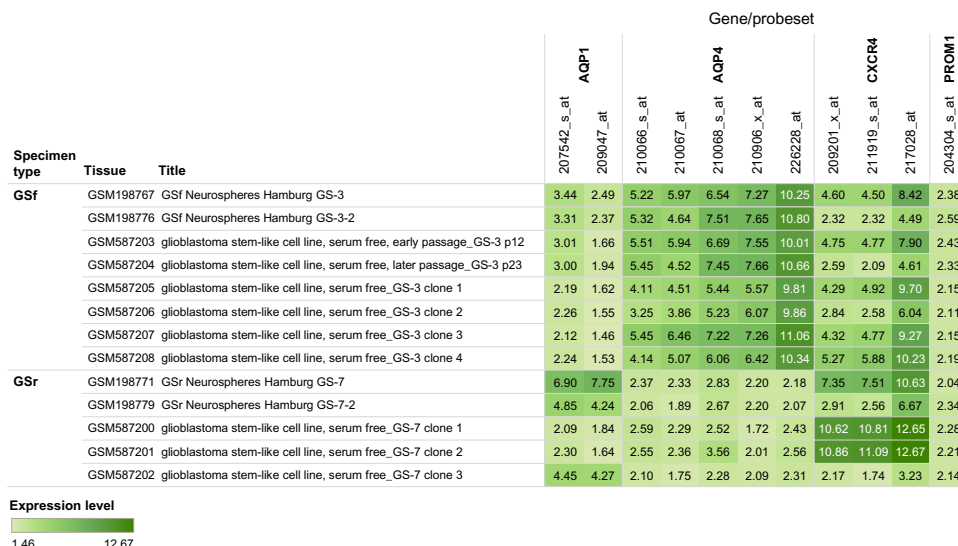


**Figure 3.** Heat map of expression levels for AQP1, AQP4, CXCR4, and PROM1 in two glioblastoma stem-like clonal sublines (GS-3 and GS-7) and their associated passaged parental lines and neurospheres. Interactive version of figure is available at [https://public.tableausoftware.com/views/glioma\\_aqp/figure3](https://public.tableausoftware.com/views/glioma_aqp/figure3).

GS-8 and GS-8-2 differed in the expression levels of PROM1 (CD133) (8.719 vs 2.600). Among the nine restricted stem-like (GSr) neurospheres, the expression level of the AQP1 probe set in four neurospheres (GS-4, GS-4-2, GS-7 and GS-7-2) was twofold more than that of the AQP4 probe set. The remaining five GS neurospheres had expression levels in which 1) AQP4

was onefold more than AQP1 (GS-1-2 and GS-2) or 2) AQP1 was onefold more than AQP4 (GS-1, GS-2-2, and GS-6). In summary, seven of the eight GSf neurospheres followed the pattern of low AQP1 and high AQP4, while in GSr neurospheres only four of the nine samples had the pattern of high AQP1 and low AQP4.



**Figure 4.** Comparison of expression levels for selected probe sets of AQP1, AQP4, CXCR4, and PROM1 in glioblastoma neurospheres. GSf, full stem-like phenotype, GS-3; GSr, restricted stem-like phenotype, GS-7. Interactive version of figure is available at [https://public.tableausoftware.com/views/glioma\\_aqp/figure4](https://public.tableausoftware.com/views/glioma_aqp/figure4).



The datasets transformed for visual analytics and statistical analysis are available as a Supplementary File to this article. A collection of visual analytics resources for performing complex cognitive activities (such as sense-making and knowledge discovery) on the datasets is available at [https://public.tableausoftware.com/views/glioma\\_aqp/abstract](https://public.tableausoftware.com/views/glioma_aqp/abstract).

**AQP1 and AQP4 expression are better predictors for tumor formation and growth types in glioblastoma than are CXCR4 and PROM1.** Figure 5 aligns the AQP expression in growth types and tumor formation. For AQP1 and AQP4, Kruskal–Wallis ANOVA retrieved highly significant differences between all categories in both tests as well as differences between AQP1 and AQP4 expression in tumor formation and growth (Table 1). Grouping expression patterns according to group mean showed that AQP1 expression in spherical growth cultures, diffuse tumors, and solid tumors was lower than in semi-adherent and adherent growth cultures, as well as in instances where no tumor was formed. Further, AQP4 expression was lower in semi-adherent and adherent cultures as well as in solid and no tumors than in diffuse tumors and spherical growth cultures.

The additionally investigated tumor markers CXCR4 and PROM1 showed low expression in primary tumors. PROM1 was not strongly expressed in all growth types and tumor formation categories, except for medium expression in the “No tumor” category. CXCR4 also had medium strength of expression in this category but uniformly high expression in all others. Discriminant Function Analysis (DFA) showed that growth type and tumor formation could be predicted with low error probabilities by candidate marker expression (Table 2). A plot of the first two canonical roots of the DFA showed that “no tumor”, “spherical”, and “adherent” could be completely discriminated. However, diffuse/solid tumor formation and semi-adherent growth by themselves were not sufficiently predictable from our dataset (Fig. 5, Table 2). The strongest were AQP1 and AQP4, followed by CXCR4. PROM1 was not a significant predictor.

Consequently, the inverse AQP1/AQP4 expression ratio could predict the formation of diffuse tumors with spherical

growth form, and no tumor formation/semi-adherent or adherent growth form in cell culture (Fig. 6). AQP1 and AQP4 expression are better predictors for tumor formation and growth types in glioblastoma than are CXCR4 and PROM1.

### Discussion

This report presents, for the first time, combined visual analytics and statistical analysis of gene expression levels of aquaporins in the two publications on the genome-wide gene expression in a large collection (92 samples) of glioblastoma stem-like cells.<sup>6,7</sup> The collection of visual analytics resources developed in this study provide an interactive cognitive activity support tool to extend that capability of researchers to perform cognitive activities including knowledge discovery and learning. The strategies in the study could be applicable to datasets from next-generation sequencing (NGS) including exome sequencing data.

The integrated data analytics approach confirmed statements in the previous publication by Schulte and colleagues.<sup>6</sup> Our focus on the 13-member aquaporin gene family revealed that inverse (high/low) expression levels in two of these aquaporin genes could be correlated with two distinct phenotypes of GS cells (Figs. 1–6). Clearly, in the neurosphere cultures (Figs. 3 and 4), low AQP1 and high AQP4 expression was characteristic for the full stem-like phenotype (GS-3 and GS-3-2), while high AQP1 and low AQP4 expression was characteristic for the restricted stem-like phenotype (GS-7 and GS-7-2). Statistical analysis using DFA provided statistical support that AQP1 and AQP4 expressions are better predictors for tumor formation and growth types in glioblastoma than are CXCR4 and PROM1 (Tables 2 and 3; Figs. 5 and 6). The biological significance of these inverse expression levels of AQP1 and AQP4 in the distinct stem-like phenotypes is not clear yet. However, under the hypoxic conditions present in tumor cells, AQP1, AQP4, and AQP9 contribute to motility, invasiveness, and edema formation and facilitate metabolism.<sup>20</sup>

Seven of the eight GSf neurospheres follow the pattern of low AQP1 and high AQP4 (Fig. 4). Since the group of GSf cell lines is a more representative model of human glioblastoma, we propose that an index of the expression levels between AQP1 and AQP4 expression levels might be a useful tool to analyze and predict glioblastoma tumor formation and growth type. The relationship is based on the expression levels of Affymetrix probe sets 209047\_at (AQP1) and 226228\_at (AQP4) in 17 glioblastoma neurosphere samples. The expression levels (Log2 gcRMA) for the eight GSf neurospheres ranged from 2.215 to 11.332 in which a cut-off level of 6.0 was observed to define the inverse relationship. We therefore propose further research in which a human glioblastoma sample that will maintain highly invasive growth *in vivo* and stem cell characteristics *in vitro* will have expression level of AQP-4 that is at least twice the expression level of AQP-1, corresponding to an AQP4/AQP1 expression ratio of 2.0 or higher.

Growth ( <i>In vitro</i> )	Tumor formation ( <i>In vivo</i> )		
	Diffuse tumor	Solid tumor	No tumor
Spherical	AQP1 LOW AQP4 HIGH	AQP1 LOW AQP4 HIGH/LOW	AQP1 LOW/HIGH AQP4 HIGH/LOW
Semi-adherent	AQP1 HIGH/LOW AQP4 LOW/HIGH	AQP1 HIGH/LOW AQP4 LOW	AQP1 HIGH AQP4 LOW
Adherent	AQP1 HIGH/LOW AQP4 LOW/HIGH	AQP1 HIGH/LOW AQP4 LOW	AQP1 HIGH AQP4 LOW

**Figure 5.** Predictive inverse expression levels of AQP1 and AQP4 in glioblastoma stem-like cells.



**Table 1.** Results of Kruskal–Wallis ANOVA for differences in aquaporin expression between different categories of tumor formation and growth type. Cell numbers refer to the cell lines; KW-H; exact p (bold if significant after Bonferroni correction).

	AQP1	AQP4
Tumor growth type	207542_s_at; 46.7703; <b>0.000001</b>	210066_s_at; 55.548; <b>0.00001</b>
	209047_at; 48.1370; <b>0.00001</b>	210067_at; 43.380; <b>0.000001</b>
		210068_s_at; 55.686; <b>0.00001</b>
		210906_x_at; 56.7227; <b>0.00001</b>
		226228_at; 67.062; <b>0.00001</b>
Tumor formation	207542_s_at; 27.4645; <b>0.00005</b>	210066_s_at; 25.4446; <b>0.0001</b>
	209047_at; 28.0147; <b>0.00004</b>	210067_at; 23.6465; <b>0.0003</b>
		210068_s_at; 28.757; <b>0.00003</b>
		210906_x_at; 29.198; <b>0.00002</b>
		226228_at; 30.537; <b>0.00001</b>

**Table 2.** Results of discriminant function analysis for tumor growth and formation using the expression of four marker genes as predictor variables. Overall statistics for tests: Growth type (five groups) Wilks' Lambda: 0.4104 approx.  $F(16,248) = 28.593$   $P < 0.0001$ ,  $N = 89$ ; Tumor formation (five groups) Wilks' Lambda: 0.3375 approx.  $F(16,251) = 31.897$   $P < 0.0001$ ,  $N = 90$ . Significant predictors are in italic font.

GENE EXPRESSION	A. GROWTH TYPE				
	WILKS' LAMBDA	PARTIAL LAMBDA	F-REMOVE	P-VALUE	R <sup>2</sup>
AVG_AQP1	<i>0.115911</i>	<i>0.354088</i>	<i>36.93911</i>	<i>0.000000</i>	<i>0.159431</i>
AVG_AQP4	<i>0.114821</i>	<i>0.357448</i>	<i>36.40155</i>	<i>0.000000</i>	<i>0.059974</i>
AVG_CXCR4	<i>0.064632</i>	<i>0.635025</i>	<i>11.63851</i>	<i>0.000000</i>	<i>0.054285</i>
PROM1_204304_s_at	0.045640	0.899280	2.26801	0.068950	0.177620
	B. TUMOR FORMATION				
	WILKS' LAMBDA	PARTIAL LAMBDA	F-REMOVE	P-VALUE	R <sup>2</sup>
AVG_AQP1	<i>0.120167</i>	<i>0.280864</i>	<i>52.48916</i>	<i>0.000000</i>	<i>0.079863</i>
AVG_AQP4	<i>0.092660</i>	<i>0.364241</i>	<i>35.78138</i>	<i>0.000000</i>	<i>0.051369</i>
AVG_CXCR4	<i>0.052789</i>	<i>0.639348</i>	<i>11.56394</i>	<i>0.000000</i>	<i>0.037846</i>
PROM1_204304_s_at	0.035919	0.939642	1.31681	0.270631	0.105617

**Table 3.** Standardized coefficients for discriminant function analysis predictor variables (canonical roots).

PREDICTOR	A. GROWTH TYPE			
	ROOT 1	ROOT 2	ROOT 3	ROOT 4
AVG_AQP1	0.680696	0.773275	-0.158776	0.01686
AVG_AQP4	0.729460	-0.490270	0.452328	0.27762
AVG_CXCR4	0.142275	-0.525564	-0.851833	0.13136
PROM1_204304_s_at	-0.097849	-0.197596	0.034161	-1.03359
Eigenvalues	7.179787	1.604498	0.345551	0.03360
Cumulative proportion of explained variance	0.783526	0.958623	0.996333	1.00000
PREDICTOR	B. TUMOR FORMATION			
	ROOT 1	ROOT 2	ROOT 3	ROOT 4
AVG_AQP1	-0.656841	0.803783	0.332771	0.037765
AVG_AQP4	-0.729174	-0.616482	0.160620	-0.355325
AVG_CXCR4	-0.309830	0.381803	-0.899456	-0.081314
PROM1_204304_s_at	0.136520	-0.416963	-0.175126	0.996402
Eigenvalues	6.783372	1.276161	0.374741	0.000398
Cumulative proportion of explained variance	0.804225	0.955524	0.999953	1.00000



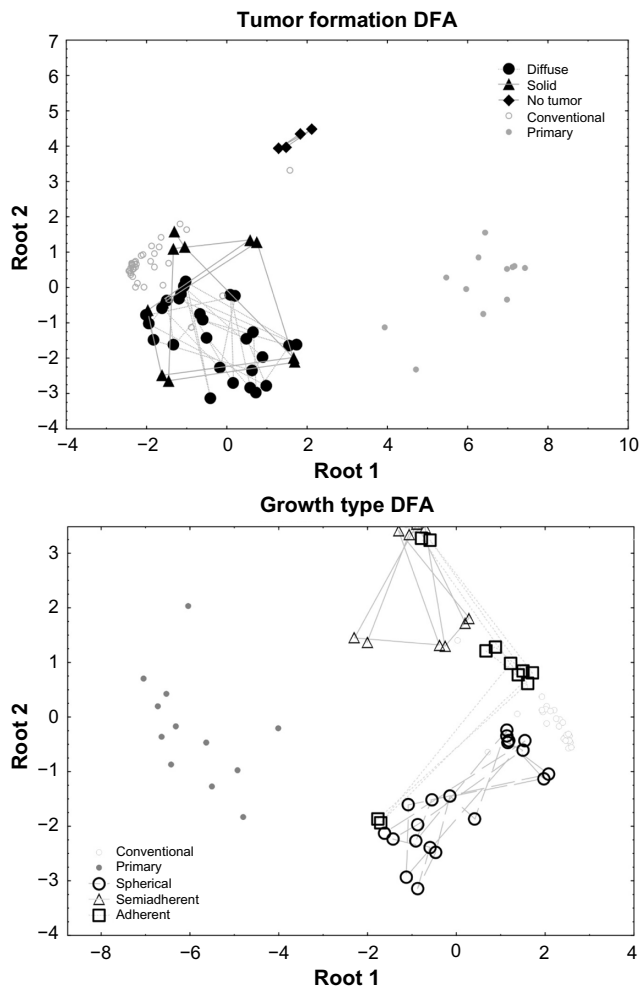


**Figure 6.** Discriminant Function Analysis (DFA) identified predictors for growth type and tumor formation in glioblastoma.

We have used expression levels obtained from Affymetrix probe sets as an indicator of gene expression. Multiple probe sets can be associated with a gene. Therefore, the statistical analysis used the average of the expression levels (Tables 2 and 3). However, there were also some clones or sub-lines of cells that had expression levels in AQP1 and AQP4 that did not fit the inverse relationship. In GS-7, clone 3 expression pattern was different from that of clones 1 and 2 (Fig. 3). The heat map revealed the high expression levels ( $>10$ ) of CXCR4 probe sets for GS-7 clone 1 and GS-7 clone 2. The difference observed could be due to the difference in CXCR4 signaling. CXCR4 is the receptor for SDF-1, a potential glioma stem cell therapeutic target.<sup>6</sup>

The combined data analytics strategy developed in this study starts with the integration of gene expression levels obtained from the BIOGPS dataset 1692 (<http://biogps.org/dataset/1692/>).<sup>16</sup> A unique contribution of the study is the transformation of the datasets in BIOGPS to formats that permit deeper insights into relationships between probe sets and expression levels. We further determined the agreement between the visual representations and the statements in a publication<sup>6</sup> on the phenotypic stability of two lineages of GS cells (GS-3 and GS-7). The method developed used visual representations

to make additional scientific discoveries from the statements in scientific publications. This form of secondary data analytics of statements in publications on glioblastoma could uncover scientific discoveries of therapeutic significance. We have previously used text mining methods to extract statements on genomic polymorphisms in arsenic-induced skin cancer.<sup>21</sup>

## Conclusions

A combination of visual analytics and statistical analysis techniques was used to uncover previously unknown relationships in a total of 2,566 expression levels from 28 Affymetrix microarray probe sets encoding 13 human aquaporins (AQP0–AQP12), CXCR4 (the receptor for SDF-1, a potential glioma stem cell therapeutic target), and PROM1 (gene encoding CD133, the widely used glioma stem cell marker). Investigations are needed to characterize the molecular mechanisms for inverse expression levels of AQP1 and AQP4 in glioblastoma stem-like neurospheres. A major novel hypothesis developed here that remains to be experimentally verified is that the AQP4/AQP1 ratio could be a diagnostic marker for distinct phenotypes of glioblastoma stem-like cells.

## Author Contributions

Conceived and designed the experiments: BG, KN, KWV, RDI. Analyzed the data: BG, KN, KWV, JNS, MP, RDI, UKU. Wrote the first draft of the manuscript: KN, KWV, JNS, RDI. Contributed to the writing of the manuscript: BG, MP, UKU. Agree with manuscript results and conclusions: BG, KN, KWV, JNS, MP, RDI, UKU. All authors reviewed and approved of the final manuscript.

## Supplementary Material

**Supplementary File 1.** This file contains additional information on data sets used in the study.

## REFERENCES

- Carbrey JM, Agre P. Discovery of the aquaporins and development of the field. *Handb Exp Pharmacol.* 2009;(190):3–28.
- Cohly HH, Isokpehi R, Rajnarayanan RV. Compartmentalization of aquaporins in the human intestine. *Int J Environ Res Public Health.* 2008;5(2):115–9.
- Fukuda AM, Badaut J. Aquaporin 4: a player in cerebral edema and neuroinflammation. *J Neuroinflammation.* 2012;9:279.
- Isokpehi RD, Rajnarayanan RV, Jeffries CD, Oyeleye TO, Cohly HH. Integrative sequence and tissue expression profiling of chicken and mammalian aquaporins. *BMC Genomics.* 2009;10(suppl 2):S7.
- Simmons SS, Isokpehi RD, Brown SD, et al. Functional annotation analytics of rhodospirillum rubrum genomes. *Bioinform Biol Insights.* 2011;5:115–29.
- Schulte A, Günther HS, Phillips HS, et al. A distinct subset of glioma cell lines with stem cell-like properties reflects the transcriptional phenotype of glioblastomas and overexpresses CXCR4 as therapeutic target. *Glia.* 2011;59(4):590–602.
- Günther HS, Schmidt NO, Phillips HS, et al. Glioblastoma-derived stem cell-enriched cultures form distinct subgroups according to molecular and phenotypic criteria. *Oncogene.* 2007;27(20):2897–909.
- Gürsel DB, Shin BJ, Burkhardt J-K, Kesavabhotla K, Schlaff CD, Boockvar JA. Glioblastoma stem-like cells – biology and therapeutic implications. *Cancers.* 2011;3(2):2655–66.
- Kyurkchiev D. Cancer stem cells from glioblastoma multiforme: culturing and phenotype. *Stem Cells.* 2014;2(1):3.
- Medema JP. Cancer stem cells: the challenges ahead. *Nat Cell Biol.* 2013; 15(4):338–44.



11. Furnari FB, Fenton T, Bachoo RM, et al. Malignant astrocytic glioma: genetics, biology, and paths to treatment. *Genes Dev.* 2007;21(21):2683–710.
12. Chen J, Xu T. Recent therapeutic advances and insights of recurrent glioblastoma multiforme. *Front Biosci.* 2013;18:676–84.
13. Clark MJ, Homer N, O'Connor BD, et al. U87MG decoded: the genomic sequence of a cytogenetically aberrant human cancer cell line. *PLoS Genet.* 2010;6(1):e1000832.
14. McCoy E, Sontheimer H. Expression and function of water channels (aquaporins) in migrating malignant astrocytes. *Glia.* 2007;55(10):1034–43.
15. Binello E, Germano IM. Targeting glioma stem cells: a novel framework for brain tumors. *Cancer Sci.* 2011;102(11):1958–66.
16. Wu C, Orozco C, Boyer J, et al. BioGPS: an extensible and customizable portal for querying and organizing gene annotation resources. *Genome Biol.* 2009;10(11):R130.
17. Isokpehi RD, Udensi UK, Anyanwu MN, et al. Knowledge building insights on biomarkers of arsenic toxicity to keratinocytes and melanocytes. *Biomark Insights.* 2012;7:127.
18. Thomas JJ, Cook KA. A visual analytics agenda. *IEEE Comput Graph Appl.* 2006;26(1):10–3.
19. Fisher B, Green TM, Arias-Hernández R. Visual analytics as a translational cognitive science. *Top Cogn Sci.* 2011;3(3):609–25.
20. Fossdal G, Vik-Mo EO, Sandberg C, et al. Aqp 9 and brain tumour stem cells. *Sci World J.* 2012;2012.
21. Isokpehi RD, Cohly HH, Anyanwu MN, et al. Candidate single nucleotide polymorphism markers for arsenic responsiveness of protein targets. *Bioinform Biol Insights.* 2010;4:99.